Remote Sensing of Environment 230 (2019) 111196

Contents lists available at ScienceDirect

Remote Sensing of Environment

journal homepage: www.elsevier.com/locate/rse

The ECOSTRESS spectral library version 1.0

Susan K. Meerdink[c,*], Simon J. Hook[b], Dar A. Roberts[a], Elsa A. Abbott[b]

[a] Department of Geography, University of California Santa Barbara, Santa Barbara, CA 93106-4060, United States
[b] National Aeronautics and Space Administration Jet Propulsion Laboratory, Pasadena, CA 91109, United States
[c] University of Florida, Gainesville, FL 32611, United States

ARTICLE INFO

Edited by Jing M. Chen

Keywords:
Spectroscopy
Visible shortwave infrared (VIS/SWIR)
Thermal infrared (TIR)
Spectral library
Non-photosynthetic vegetation (NPV)
Vegetation

ABSTRACT

In June 2018, the ECOsystem Spaceborne Thermal Radiometer Experiment on Space Station (ECOSTRESS) mission was launched to measure plant temperatures and better understand how they respond to stress. While the ECOSTRESS mission delivers imagery with ~60 m spatial resolution, it is often useful to have spectra at the leaf level in order to explain variability seen at the pixel level. As it was originally titled, the Advanced Spaceborne Thermal Emission Reflection Radiometer (ASTER) spectral library version 2.0 has been expanded to support ECOSTRESS studies by including major additions of laboratory measured vegetation and non-photosynthetic vegetation (NPV) spectra. The library now contains 541 leaf visible shortwave infrared (VIS/SWIR) spectra, 472 leaf thermal infrared (TIR) spectra, and 51 NPV VIS/SWIR and TIR spectra. Previously, the library primarily contained VSWIR and TIR laboratory spectra of minerals, rocks, and man-made materials. This new library, containing over 3000 spectra, was renamed the ECOSTRESS spectral library version 1.0 and is publicly available (http://speclib.jpl.nasa.gov). It should be noted that as with the prior versions of the library, the VSWIR and TIR measurements were made with separate instruments with different calibration sources. Care should be taken when combining the data into a seamless spectrum to cover the entire spectral range. The ECOSTRESS spectral library provides a comprehensive collection of natural and man-made laboratory collected spectra covering the wavelength range of 0.35–15.4 μm.

1. Introduction

In 2018, the ECOsystem Spaceborne Thermal Radiometer Experiment on Space Station (ECOSTRESS) was deployed on the International Space Station (ISS) with the primary goal of measuring plant temperatures in order to understand how much water plants need and how they respond to stress. ECOSTRESS provides data with a 38-m in-track by 69-m cross-track spatial resolution and five spectral bands in the 8–12.5 μm range with an additional band at 1.6 μm for geolocation (Hulley et al., 2017). The Noise Equivalent Delta Temperature (NEdT) is ≤0.15 K in 3 of the 5 bands and ≤0.35 K in the remaining bands. In order to understand the variability seen at these pixel sizes, it is often useful to examine leaf spectral variability. However, leaf spectra, especially in the TIR spectra, are not commonly available or only in small sample sizes. To assist researchers in addressing the ECOSTRESS science goals, laboratory spectra of vegetation and non-photosynthetic vegetation (NPV) in the visible/shortwave-infrared (VIS/SWIR; 0.35–2.5 μm) and thermal (TIR; 2.5–15 μm) spectral range are needed. Existing spectral libraries are limited in assisting this mission either by a lack of NPV spectra or TIR spectra of plant materials.

Due to the important role ecosystems play in climate, hydrologic cycles, and biogeochemical cycles it is not surprising that many researchers have focused on vegetation spectra to get unique insights into plant traits and function (Bonan, 2013). However, NPV also plays an important role as a major proportion of biomass in dormant plant communities, an indicator of plant stress, as well as a measure of wildfire fuel conditions and biosphere-atmosphere interactions such as the carbon cycle (Elvidge, 1990; Roberts et al., 2003; Schimel et al., 2014). It can also be a confounding factor in remote sensing applications and is particularly difficult to distinguish from soils (Roberts et al., 1993). NPV, such as dry leaf litter, bark, wood, and stems, contributes to the reflectance of many terrestrial surface and varies both spatially and seasonally (Elvidge, 1990). Depending on the canopy composition and structure, NPV materials have been found to significantly influence the vegetation signature primarily in the near-infrared (Asner, 1998).

There are many spectral libraries that contain VIS/SWIR data for vegetation and NPV, but few contain spectra in both the VIS/SWIR and TIR. Previously, high spectral resolution TIR data have been limited due to the paucity of sensors while low signal to noise ratios have tended to obscure the subtle TIR features of plants (Ribeiro Da Luz and Crowley,

* Corresponding author.
E-mail address: susanmeerdink@ufl.edu (S.K. Meerdink).

https://doi.org/10.1016/j.rse.2019.05.015
Received 29 October 2018; Received in revised form 25 March 2019; Accepted 12 May 2019
Available online 22 May 2019
0034-4257/

2007). However, technological advances have allowed more studies to explore how hyperspectral TIR data can be used in vegetation research (Fabre et al., 2011; Meerdink et al., 2016; Ribeiro Da Luz and Crowley, 2007, 2010; Ullah et al., 2012b). With the development of the Hyperspectral Thermal Emission Spectrometer (HyTES) airborne instrument, hyperspectral airborne data are now becoming widely available. Together, with the launch of ECOSTRESS and the possibility of large scale VIS/SWIR and TIR spectra of vegetation, full spectrum spectral libraries with complete metadata will be required to characterize the variation seen in imagery.

To support ECOSTRESS activities, the Advanced Spaceborne Thermal Emission Reflection Radiometer (ASTER) spectral library has been updated and renamed the ECOSTRESS spectral library version 1.0. The updated library represents a significant increase from the original four vegetation spectra and now contains 541 vegetation VIS/SWIR spectra, 472 vegetation TIR spectra, and 51 NPV VIS/SWIR and TIR spectra. The ECOSTRESS spectral library 1.0 has over 3000 spectra of lunar and terrestrial soils, man-made materials, meteorites, minerals, NPV, rocks, vegetation, and water/snow/ice. In this paper, we summarize the collection, measurement, and metadata changes that are present in the new ECOSTRESS spectral library. Specifically, we will discuss the addition of over 540 vegetation spectra and 50 NPV spectra.

2. Methods

2.1. ASTER spectral library

Situated on NASA's Terra platform, ASTER is a multi-spectral imager that provides observations in the visible and near infrared (0.4–1.0 μm), the shortwave infrared (1.0–2.4 μm), and the thermal infrared (8–12 μm). To support ASTER research, a spectral library was compiled with 2400 natural and man-made materials contributed from the Jet Propulsion Laboratory, Johns Hopkins University, and the United States Geological Survey. Measured materials include ice, lunar soils, man-made materials, meteorites, minerals, rocks, snow, terrestrial soils, and vegetation. The library contains laboratory spectra measured from two wavelength ranges: 0.35–2.5 μm and 2.5–15.4 μm. The latest version of the library was released in December 2008 and described in Baldridge et al., 2009. As of February 2018, 7155 copies of the ASTER spectral library have been distributed around the world. Since the ECOSTRESS library went live in February 2018 to August 2018, 645 copies have been distributed. The new ECOSTRESS spectral library contains all spectra collected as part of the ASTER spectral library together with 1116 vegetation and NPV VIS/SWIR and TIR spectra. Metadata fields for the above-mentioned materials from the ASTER spectral library have been preserved with a few changes in formatting to match the new files. Table 1 compares metadata fields for different materials in the ECOSTRESS spectral library. The ASTER file naming conventions have been altered and are described in the library organization section. The ASTER spectral library files were inspected and updated to fix any errors that were found in metadata, spectra, and formatting.

2.2. Sample collection and preparation

The new spectra were obtained from samples that were collected as part of three projects that were not directly funded to support the ECOSTRESS mission. These samples are predominately focused on species in southern California due to proximity of the National Aeronautics and Space Administration (NASA) Jet Propulsion Laboratory (JPL) and the lab spectrometers necessary for measurements. The spectra in the library are collected from leaves and are not fully representative of canopy measurements. For more information on scaling from leaf to canopy measurements, please refer to the Discussion Section.

The first project collected fresh leaves from sixteen common California shrub and tree species in the 2013 spring, summer, and fall seasons (Meerdink et al., 2016). The 284 samples exhibited a wide range of leaf traits as determined by standard analytical procedures: 4.2–27.3% for cellulose, 2.6–22.5% for lignin, 34.7–388.9 g/m^2 for leaf mass per area, 0.45–3.81% for nitrogen, and 20.2–76.9% for water content. These plant samples were collected from three different sites within California, United States: coastal Santa Barbara County, interior Santa Barbara County, and the Sierra Nevada Mountains. The second project, Meerdink et al. (2019), collected fresh leaf samples from the Huntington Botanical Gardens, located in San Marino, CA, USA and Los Angeles Arboretum, located in Arcadia, CA, USA. This project measured leaf samples from seventy species (206 samples total) in conjunction with the HyTES sensor being flown over the Huntington Botanical Gardens. The final project collected fresh leaf samples from eleven Harvard Forest plant species and non-photosynthetic leaf samples from the same study sites as Meerdink et al. (2016). Harvard forest samples were collected to provide a better understanding of emissivity differences between plant species and plant materials (leaves and bark) to improve temperature retrievals from FLIR TIR camera systems (Aubrecht et al., 2016).

All samples from the three above-mentioned projects were processed with the same procedure. Fresh leaf samples were harvested in the field and spectral measurements conducted in the lab. Fresh leaf samples were collected from tree species using pole clippings and from shrub species using pruning shears. Multiple leaves were collected from individual plants, with leaves randomly selected from the highest accessible part of the canopy. For taller individuals this means that sampled leaves received full sun for part of the day, whereas leaf samples from shorter individuals were collected from the top of the canopy in full sun exposure. The fresh leaf samples were placed in polyethylene bags with damp paper towels and stored in a cooler at ~10 °C with a towel to prevent direct contact with ice. NPV samples were placed in polyethylene bags without a damp paper towel.

In order to preserve the integrity of the samples, spectra were measured at the NASA Jet Propulsion Laboratory within 48 h of collection. Before spectral analysis, leaves were removed from polyethylene bags and excess moisture wiped off. If a single leaf did not fill the field of view, multiple leaves from the same individual were clustered while minimizing gap and overlap between leaves. TIR spectra were measured first because these measurements are less destructive compared to the heat load of Analytical Spectra Device (ASD) measurements. Leaves were placed on aluminum foil to isolate the sample

Table 1
Metadata fields for sample types.

Line number	Mineral, rock, man-made, soil, lunar, and meteorite	Vegetation and non-photosynthetic
1	Name	Name
2	Type	Type
3	Class	Class
4	Subclass	Genus
5	Particle Size	Species
6	Sample No.	Sample No.
7	Owner	Owner
8	Wavelength Range	Wavelength Range
9	Origin	Origin
10	Collection Date	Collection Date
11	Description	Description
12	Measurement	Measurement
13	First Column	First Column
14	Second Column	Second Column
15	X Units	X Units
16	Y Units	Y Units
17	First X Value	First X Value
18	Last X Value	Last X Value
19	Number of X Values	Number of X Values
20	Additional Information	Additional Information
21	Empty Space	Empty Space
22	Spectrum Starts	Spectrum Starts

and minimize heating (Ribeiro Da Luz and Crowley, 2007). The aluminum foil could result in elevated reflectance values if gaps were present for samples that did not fill the field of view or if energy was transmitted from the aluminum foil through the leaf. Care should be taken with the interpretation of dry plant material which may transmit some radiation. Next, the same leaves were transferred to a < 5% reflective black background mat for VIS/SWIR measurements. The reflectance from the adaxial leaf surfaces is reported in the ECOSTRESS spectral library.

2.3. Sample measurement

The ECOSTRESS library contains spectra collected across two wavelength ranges: VIS/SWIR (0.35–2.5 μm) and TIR (2.5–15.4 μm). Multiple instruments were used to obtain spectra across this entire region including an Analytical Spectra Device (ASD) Field Spec 3 Spectrometer, a Beckman UV5240 Spectrophotometer, a Nicolet 520FT-IR Spectrometer with Labsphere integrating sphere, and a Perkin-Elmer Lambda 900 UV/VIS/NIR Spectrophotometer. For all NPV spectra and most vegetation spectra added to the ASTER spectral library, only the ASD and Nicolet instrument were used to collect the 0.35–15.4 μm spectral range. Due the use of two different sensors in order to measure reflectance from 0.35 to 15.4 μm, there can be a discontinuity between spectral ranges. For more information about the discontinuity and addressing the gap before combining the two sensor's measurements, please refer to the Discussion Section. See Baldridge et al., 2009 for Beckman and Perkin-Elmer instrument methodology.

The ASD Field Spec 3 Spectrometer measures 2151 contiguous channels over the 0.35–2.5 μm range (Analytical Spectra Devices, Inc., Boulder, CO, USA). The ASD full width half maximum (FWHM) at 0.7 μm is 0.003 μm, at 1.4 μm is 0.01 μm, and at 2.1 μm is 0.01 μm. The sensor's original sampling interval is 0.0014 μm for the spectral region 0.35–1.0 μm and 0.002 μm in the 1.0–2.5 μm range, and is interpolated to a finer sampling interval of 0.001 μm. To illuminate samples, a calibrated quartz halogen light source was positioned 23 cm from the target and at a 23° zenith angle. Spectra were collected using the bare fiber that was positioned at a distance of 5 cm from the target with a 27° view zenith. This configuration produces a 1.5 cm diameter field of view with a 50° phase angle and bi-directional reflectance. Each spectrum collected by the ASD is the average of ten scans. Spectralon was used as a calibrated reflectance standard to convert from raw radiance to absolute reflectance (Labsphere Inc., Durham, NH). Each sample was an average of approximately fifteen spectra, which were collected in one of two ways. In the first approach, a single set of leaves had five spectra collected repeatedly with leaves being rotated in between each set of five until fifteen spectra were collected or leaves experienced heat overload. In the second approach, five spectra were collected for three different sets of leaves from the same individual. The method that was used for a specific sample is located in the sample's auxiliary file or metadata description line in the ECOSTRESS spectral library. Samples measured with the ASD underwent quality assurance through visual assessment and were averaged so that one sample had one spectrum using code located at https://github.com/susanmeerdink/ASD-Nicolet-Spectra-Processing.

The Nicolet 520FT-IR Spectrometer fitted with a Labsphere gold coated integrating sphere (model RSA N1 700D) measures reflectance from 2.5 to 15.4 μm (Thermo Electron Corp., Madison, WI, USA). This sensor uses a single EverGlo infrared light source that has a bulb temperature of 1140 °C to output constant radiation. To reduce the impact of moisture in the air on the spectra, dry air was sent into the external sphere. Gold was measured once an hour and used as a standard to calibrate the Nicolet. Distilled water was used to check the calibration and accuracy of reflectance products (Hecker et al., 2011). The Nicolet has a sampling interval of 0.001 μm and each spectrum was determined from 300 scans that took approximately three minutes to collect. Each sample was an average of three spectra, which were collected using the same approached as the VIS/SWIR component either as a sample of a single set of leaves rotated three times or three sets of different leaves from the same individual. The sample's auxiliary file or description metadata specifies which method was used. In order to report one spectrum per sample and remove low quality spectra, vegetation and NPV Nicolet samples also underwent quality assurance through visual assessment and were averaged using code located at https://github.com/susanmeerdink/ASD-Nicolet-Spectra-Processing. This sensor was used to collect spectra using slightly different methodology than materials in the ASTER spectral library 2.0. See Baldridge et al. (2009) for details.

2.4. Library organization

For each sample, a text file containing both the metadata and the spectrum was generated. The first twenty lines of the text file are dedicated to metadata information specific to that sample. Those lines contain information such as the sample name, type, class, genus, species, wavelength range, and origin. Table 1 designates what metadata fields are included for each sample class type and the corresponding line in the text file. The header tag for lines four and five have been altered from the original ASTER spectral library to be more appropriate for vegetation and NPV samples. Following the twenty lines dedicated to the metadata, each line contains two values: wavelength and the reflectance value at that specific wavelength. See Table 2 for an example of an entire file.

Each file is assigned a unique name. For mineral and rock samples, the filename describes the type, class, subclass, particle size,

Table 2
Example of an ECOSTRESS spectrum file. Each file comprises of 20 lines of metadata and one spectrum. Filename is vegetation.tree.quercus.agrifolia.tir.vh172.ucsb.nicolet.spectrum.txt.

Name: *Quercus agrifolia* 1
Type: vegetation
Class: tree
Genus: Quercus
Species: agrifolia
Sample No.: VH172
Owner: UCSB
Wavelength Range: TIR
Origin: 34.7153; −120.0601; WGS84
Collection Date: 6/9/2013
Description: Samples were collected as part of the HyspIRI Airborne Campaign. 48 individual plants were sampled in three times in 2013 - spring, summer, and fall. The name of the sample includes a 1, 2, or 3, which references a different individual of the species. Samples were taken to JPL and processed within 48 h of collection. The same leaves were processed in the Nicolet and then measured using the ASD.
Measurement: Directional hemispherical reflectance
First Column: X
Second Column: Y
X Units: Wavelength (micrometers)
Y Units: Reflectance (percentage)
First X Value: 2.501
Last X Value: 15.387
Number of X Values: 1737
Additional Information:
vegetation.tree.quercus.agrifolia.tir.vh172.ucsb.nicolet.ancillary.txt

2.5010 9.2470
2.5030 9.3250
2.5040 9.4810
2.5050 9.3120
2.5060 9.2130
2.5070 9.3840
2.5090 9.4740
2.5100 9.2740
2.5110 9.1190
2.5120 9.0330
* Wavelength and Spectrum Data Continues *

Table 3
Library nomenclature examples.

Type	Mineral, rock, man-made, soil, lunar, meteorite, vegetation, non photosynthetic vegetation
Class	Silicate, Sulfate, Carbonate, Sedimentary, Igneous, Tree, Shrub, Branches, Dry Needles, Grasses, Bark
Subclass or genus	Subclass Examples: Phyllosilicate, Tectosillicate, Felsic, Mafic Genus Examples: *Acer, Bambusa, Quercus, Avena, Arctostaphylos, Ceanothus*
Particle size or species	Particle Size Examples: Solid, Fine, Medium, Coarse Species Examples: *paxii, beecheyana, agrifolia, fatua, glandulosa, spinosus*
Wavelength range	VIS/SWIR, TIR
Sample number	
Owner	JPL, JHU, UCSB, USGS
Instrument	ASD, Beckman, PerkNic, Nicolet
File Type	Spectrum, Ancillary

Mineral Example: mineral.sulfate.none.coarse.VIS/SWIR.so-1a.jpl.perkin.spectrum.txt.
Vegetation Example: vegetation.shrub.salvia.leucophylla.tir.vh095.ucsb.nicolet.spectrum.txt.

wavelength range, sample number, owner of spectra, and spectrometer used. For vegetation and NPV, the filename describes the sample type, class, genus, species, wavelength range, sample number, owner of spectra, and ends with the spectrometer used. The spectral files are given the suffix "spectrum.txt". For example, the spectrum of *Quercus agrifolia* measured at JPL on the Nicolet will have the filename "vegetation.tree.quercus.agrifolia.all.VH172.jpl.Nicolet.spectrum.txt". Some samples have an optional, ancillary text file that contains information that is not part of the standard spectral file format such as leaf trait properties. The ancillary data files are given the suffix "ancillary.txt". The naming convention is further explained and examples are shown in Table 3.

2.5. Ordering the library

The complete ECOSTRESS spectral library is available for download as a single zip file from http://speclib.jpl.nasa.gov/. This file contains data that are uniquely named text files as noted in the library organization section. On the Download Tab, users have the option of selecting portions of the library or the entire library. On the Search Library Tab, individual spectra can also be searched, viewed, and downloaded online.

3. Results and discussion

The 2.0 version of the ASTER spectral library was comprised of over 2400 spectra including: 1748 minerals, 473 rocks, 69 soils, 17 lunar materials, 60 meteorites, 4 vegetation, 9 water/snow/ice, and 84 man-made materials (Baldridge et al., 2009). The ECOSTRESS library combines these existing spectra with additional vegetation and NPV spectra to include over 450 vegetation spectra representing 90 species and 51 NPV spectra including bark, dry needles, lichen, and dry leaves. The ECOSTRESS spectral library is the only publicly accessible library that contains both the VIS/SWIR (0.35–2.5 μm) and TIR (2.5–15 μm) spectral signatures for vegetation and NPV.

Vegetation spectra in the 0.35–2.5 μm spectral range share common absorption features as seen in the example vegetation spectra from the library in Fig. 1 (Curran, 1989). The 0.4–0.7 μm spectral range is dominated by chlorophyll absorption features that result in a characteristic increase in reflectance around 0.55 μm giving plants their green color to human eyes (Woolley, 1971). All plants exhibit a large increase in reflectance around 0.7 μm as they transition from strong chlorophyll absorption to near infrared scattering known as the red-edge (Horler et al., 1983). In the near infrared, there is high reflectance due to scattering from internal leaf structures. Additionally, all species have four major water absorption features at 0.97, 1.20, 1.40, and 1.94 μm (Curran, 1985; Danks et al., 1983). Across the VIS/SWIR spectrum, the spectral differences between samples and species are the result of variations in biochemical and biophysical traits such as cellulose, chlorophyll, leaf thickness, leaf structure, lignin, nitrogen, oil, proteins, sugar, and water content (Asner and Martin, 2016; Curran, 1989). VIS/SWIR spectroscopy has been leveraged for numerous vegetation research objectives such as monitoring invasive species expansion (Underwood et al., 2003), tracking wildfire disturbance recovery (Riaño et al., 2002), mapping plant functional types (Ustin and Gamon, 2010), determining plant traits and morphology (Serbin et al., 2014), and detecting vegetation disasters such as insect infestation (Lawrence and Labus, 2003).

In the 2.5–15 μm spectral range, vegetation samples have subtle spectral features and generally low reflectance. This low reflectance is attributed to the intense TIR absorption caused by liquid water and organic compounds present in fresh leaf tissues. Higher reflectance values were generally found on leaves having copious hair, thick waxy cuticles, or lower water content (Salisbury, 1986; Salisbury and Milton, 1988). An example of increased reflectance values for decreasing water content is shown in Fig. 2 for *Quercus douglasii*, a broadleaf deciduous tree, and *Salvia leucophylla*, a drought deciduous shrub. In the TIR, green leaves are opaque and reflectance is primarily the product of the leaf cuticle and the underlying cell wall (Ribeiro Da Luz and Crowley, 2007). Cuticular structures may be unique between plant species and can be treated as a species identifier (Holloway, 1982). Species-specific waxy cuticle composition has been found to uniquely influence the spectral signature in this wavelength region (Heredia-guerrero et al., 2016; Ribeiro Da Luz and Crowley, 2007). Additional work conducted by Ribeiro da Luz and Crowley (2007) found spectral features in the TIR (8–14 μm) associated with cellulose, cutin, xylan, silica, and oleanolic acid. By contrast, leaf reflectance in the VIS/SWIR is the product of the internal leaf structure, and plant biochemicals such as water, pigments and structural and components such as lignin and cellulose (Curran, 1989; Gates and Tantraporn, 1952; Salisbury, 1986; Wong and Blevin, 1967). As leaf water content decreases, reflectance generally increases in the VIS/SWIR (Hunt and Rock, 1989), although NIR reflectance can decrease in senescing leaves (Elvidge, 1990), as shown for *Salvia leucophylla.* TIR reflectance (8–14 μm) shows a modest increase in reflectance with decreasing water content (< 5%), with larger increases observed in *Quercus* that are similar in magnitude as those reported by Gerber et al. (2011) for *Cercis Canadensis* (Fig. 2). At shorter wavelengths (3–5 μm), a much greater increase in leaf reflectance is observed with a decrease in water content, consistent with observations from Gerber et al. (2011). While, TIR spectra have not been used extensively in the literature, they have been used for species discrimination (Ribeiro Da Luz and Crowley, 2010; Ullah et al., 2012a) and water content retrieval (Fabre et al., 2011; Meerdink et al., 2016; Ullah et al., 2012b).

NPV leaf materials in the VIS/SWIR spectral range bear little resemblance to those of green leaves because both chlorophyll and water are lost during leaf senescence (Fig. 3; Elvidge, 1990). In NPV, chlorophyll has degraded resulting in a higher reflectance in the 0.4–0.7 μm region compared to fresh leaf samples which have strong chlorophyll absorption at these wavelengths (Elvidge, 1990). NPV materials lose the

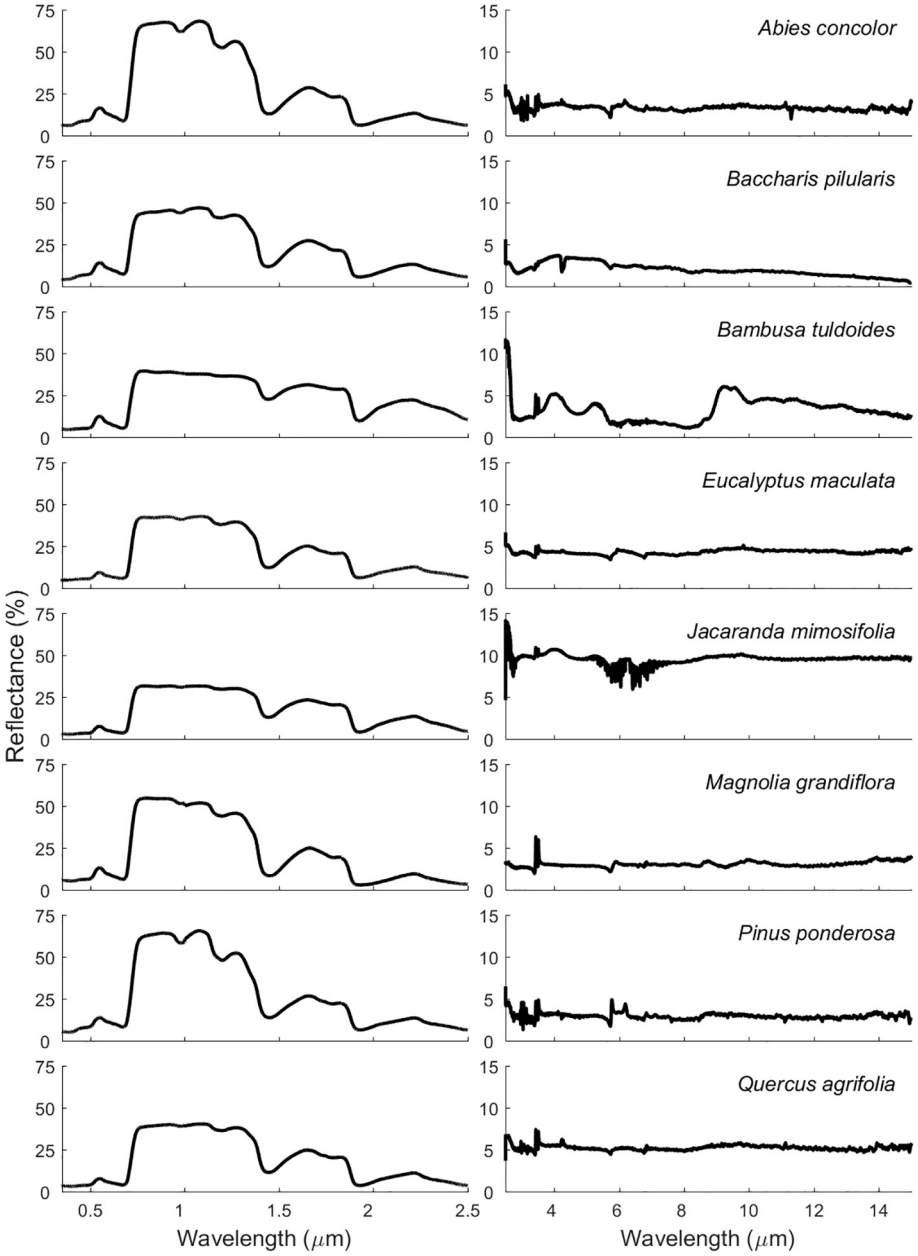

Fig. 1. Examples of vegetation reflectance spectra of several species across the visible/shortwave infrared (0.35–2.5 μm) and thermal infrared (2.0–15.4 μm) wavelength ranges. Vertical scaling differs between the VIS/SWIR and TIR to accentuate subtle spectral differences in the TIR.

characteristic red-edge that is present in green leaf samples due decreasing water content and the changing internal leaf structure (Fig. 3). Beyond 1.0 μm, spectra are dominated by strong absorption features caused by lignin and cellulose concentrations that are generally obscured by water content in green leaf samples (Curran, 1989). NPV can be spectrally similar to soil, except for the presence of lignin and cellulose absorption features (Roberts et al., 1993). NPV materials such as bark and branches exhibit similar spectroscopy patterns compared to low water content NPV leaf materials. Bark and branch reflectance signatures have strong lignin and cellulose absorption features (Kozhoridze et al., 2016). NPV spectroscopy is used frequently for subpixel mapping and fractional cover estimates in a variety of ecosystems (Okin et al., 2001; Roberts et al., 1998; Wetherley et al., 2017).

In the 2.5–15 μm spectral range, NPV spectral signatures have higher reflectance between 4 and 6 μm than fresh leaf samples mainly due to lower water content (Fig. 3). Without water to mask the signal, NPV leaf spectra express stronger absorption features as a result of the composition of the cuticle and cell walls, specifically lignin, cellulose, and hemicellulose (Elvidge, 1988). NPV exhibits intense absorption in the 3.0 μm region and have their highest reflectance in the 4.0–5.5 μm range, whereas green leaves have a low reflectance in this range due to intense leaf water absorption. This pattern is also present in bark and branch NPV samples due to high concentrations of lignin and cellulose (Kozhoridze et al., 2016). Although green leaves and NPV generally appear to have good separability between 3 and 5 μm, this region is complicated due to the long wavelength edge of the solar radiation curve and the short wavelength edge of the terrestrial emittance curve when working at airborne or space-borne scales (Gates et al., 1965).

For many samples in the library, a VIS/SWIR and TIR spectrum is available but a discontinuity in spectra is present at 2.5 μ. For a majority of samples there is less than a 5% difference in reflectance between sensors, but this discontinuity can be as large as 15–20% difference in reflectance (present in 16 samples). These differences are to be expected and related to four key differences between two

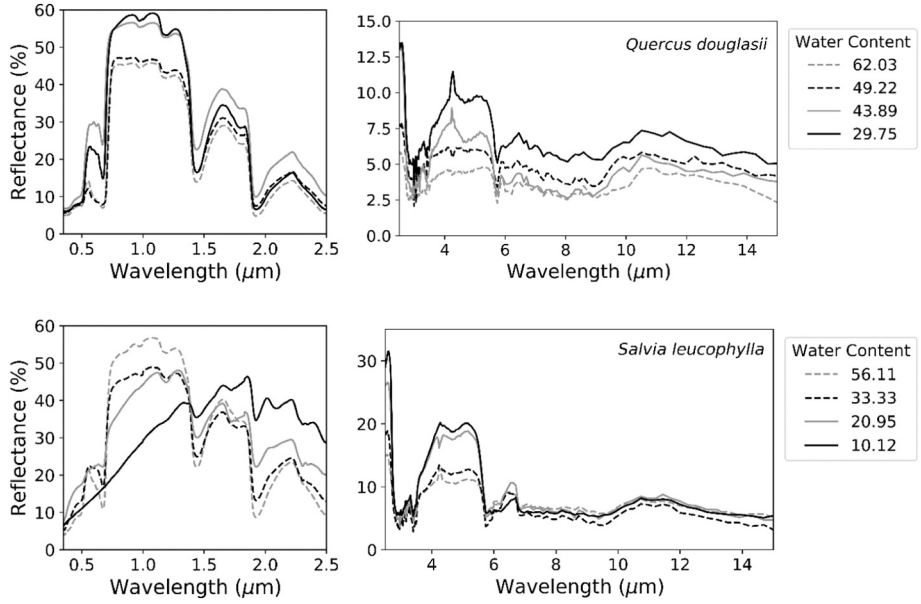

Fig. 2. Changes in reflectance in the VIS/SWIR and TIR spectrum for two species with changes in water content: *Quercus douglasii* (on top) and Salvia leuchophylla (on bottom). Minor spikes or troughs centered at 4.3 μm are due to residual carbon dioxide and when present, these wavelengths should be removed.

spectrometers the VIS/SWIR and TIR measurements. First, the ASD and Nicolet use different standards (spectralon versus gold) for calibration, which guarantees the spectra will not match in the overlap zone since neither standard is a perfect reflector in the overlap zone. Secondly, the signal to noise ratio of spectrometers decreases at the upper and lower ends of the instruments sampling range. Thirdly, the Nicolet measurements are purged and therefore have a different atmosphere above the sample. Lastly, the ASD and Nicolet represent measurements under different lighting and viewing geometry conditions. For example, the ASD measurements are bidirectional and involve a quartz halogen light source while the Nicolet measurements are directional hemispherical with a directional light source and integrating sphere.

There are a few methods for correcting the sensor discontinuity. For example, Veraverbeke et al. (2012) applied an amplitude translation to the TIR to match VIS/SWIR reflectance for the same materials. Gerber et al. (2011) developed a physically based correction that took advantage of overlap between the VIS/SWIR and TIR sensors from 2 to 2.5 μm to address the gap. This approach also incorporated transmittance and reflectance from four PolyTetraFluoroEthylene standards with variable thickness. No overlap occurs in the vegetation and NPV samples described in this manuscript, and the sensors were not configured to enable transmittance measurements. To account for the gap, spectra are delivered separately in the VIS/SWIR and TIR to allow users to apply a preferred correction should they choose to merge the two wavelength regions.

The ECOSTRESS spectral library only contains vegetation spectra from leaf samples. In the VIS/SWIR, leaf spectra deviate from canopy spectra due to influences of canopy structure, the presence of NPV, background substrate, and multiple scattering within the canopy (Asner and Martin, 2008; Ollinger, 2011; Roberts et al., 2004; Verhoef, 1984). Scaling in the TIR is complicated because several factors weaken the already subtle plant features including canopy voids, leaf angle, canopy structure, and errors in temperature emissivity separation retrievals (Ribeiro Da Luz and Crowley, 2007, 2010; Salisbury, 1986). Radiative transfer models have been used extensively in the literature to scale leaf level measurements to canopy level in the VIS/SWIR domain (Gobron et al., 1997; Iaquinta and Pinty, 1997; Jacquemoud et al., 2000; Kuusk, 1995; Verhoef, 1984) and the TIR domain (Francois et al., 1997; Jacob et al., 2017; Olioso, 1995; Snyder and Wan, 1998; Verhoef et al., 2007).

With the addition of vegetation and NPV spectra, spectral library applications can be expanded to support upcoming missions such as the international space station ECOSTRESS mission that was delivered to the International Space Station in June 2018. The existing spectral library has already been widely used in many applications such as geological mapping, land surface temperature and emissivity retrieval, urban environment measurements, and carbon dioxide estimation (Hulley and Hook, 2011; Li et al., 2013; Mitraka et al., 2012; Saitoh et al., 2009; van der Meer et al., 2012). The ECOSTRESS spectral library contains both VIS/SWIR and TIR spectral signatures which can support missions including the space-borne Hyperspectral InfraRed Imager (HyspIRI) (Lee et al., 2015), the space-borne Environmental Mapping and Analysis Program (EnMAP) (Stuffler et al., 2007), the air-borne Hyperspectral Thermal Emission Spectrometer (HyTES) (Hook et al., 2013), and the air-borne National Ecological Observatory Network (NEON) (Kampe et al., 2010). Currently the library is dominated by southern California plant species due to the scope of the projects involved and the proximity to lab spectrometers. Future versions of the library will expand the collection of species and materials for a better representation of the scope of the ECOSTRESS mission.

4. Conclusions

The ECOSTRESS spectral library 1.0 contains over 3000 spectra, including all the spectra originally found in the ASTER spectral library as well as major additions to the vegetation and NPV spectra. This library includes spectra of minerals, rocks, lunar and terrestrial soils, man-made materials, meteorites, vegetation, NPV, snow, and ice and is one of the most comprehensive collections of spectra covering the wavelength range 0.35–15.4 μm publicly available.

Acknowledgements

A portion of this work was carried out at the Jet Propulsion Laboratory/California Institute of Technology, Pasadena, California, under contract with the National Aeronautics and Space Administration. Thank you to the Huntington Gardens, specifically Sean Lahmeyer and David Sivertsen, for their support in collecting leaf samples and sharing data. We wish to thank Cibele Amaral, Carla D'Antonio, Paul Gader, Bill Johnson, Frank McDonough, Gerardo Rivera, Erin Wetherley, and Kara Youngentob for all their help in

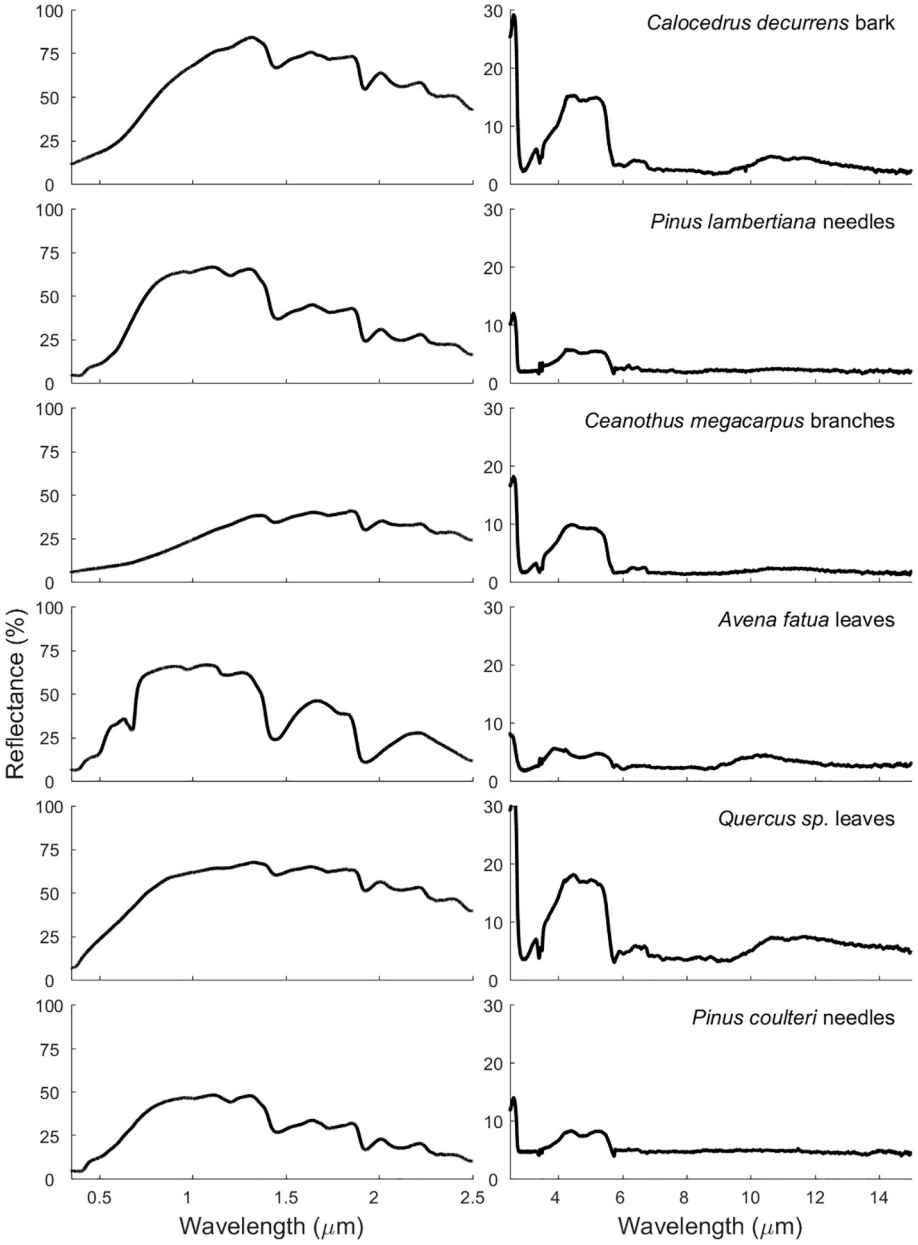

Fig. 3. Examples of non-photosynthetic vegetation (NPV) reflectance spectra of several materials across the visible/shortwave infrared (0.35–2.5 μm) and thermal infrared (2.0–15.4 μm) wavelength ranges. Minor spikes or troughs centered at 4.3 μm are due to residual carbon dioxide and when present, these wavelengths should be removed.

getting the data, website, and paper prepared. Susan Meerdink performed work while at the University of California, Santa Barbara. This project was funded as a NASA JPL Subcontract titled "*Plant species mapping, water, and LMA using HyTES"*, NASA Grant NNX12AP08G, *HyspIRI discrimination of plant species and functional types along a strong environmental-temperature gradient*, and NASA Earth and Space Science Fellowship (NESSF).

References

Asner, G.P., 1998. Biophysical and biochemical sources of variability in canopy reflectance. Remote Sens. Environ. 64, 234–253.

Asner, G.P., Martin, R.E., 2008. Spectral and chemical analysis of tropical forests: scaling from leaf to canopy levels. Remote Sens. Environ. 112, 3958–3970. https://doi.org/10.1016/j.rse.2008.07.003.

Asner, G.P., Martin, R.E., 2016. Spectranomics : emerging science and conservation opportunities at the interface of biodiversity and remote sensing. Glob. Ecol. Conserv. 8, 212–219. https://doi.org/10.1016/j.gecco.2016.09.010.

Aubrecht, D.M., Helliker, B.R., Goulden, M.L., Roberts, D.A., Still, C.J., Richardson, A.D., 2016. Continuous, long-term, high-frequency thermal imaging of vegetation: uncertainties and recommended best practices. Agric. For. Meteorol. 228–229, 315–326. https://doi.org/https://doi.org/10.1016/j.agrformet.2016.07.017.

Baldridge, A.M., Hook, S.J., Grove, C.I., Rivera, G., 2009. The ASTER spectral library version 2.0. Remote Sens. Environ. 113, 711–715. https://doi.org/10.1016/j.rse.2008.11.007.

Bonan, G., 2013. Ecological Climatology: Concepts and Applications.

Curran, P.J., 1985. Principles of Remote Sensing. Longman, New York, NY.

Curran, P.J., 1989. Remote sensing of foliar chemistry. Remote Sens. Environ. 30, 271–278. https://doi.org/10.1016/0034-4257(89)90069-2.

Danks, S.M., Evans, E.H., Whittaker, P.A., 1983. Photosynthetic Systems: Structure, Function, and Assembly. John Wiley & Sons, New York, NY.

Elvidge, C.D., 1988. Thermal infrared reflectance of dry plant materials: 2.5-20.0. Remote Sens. Environ. 26, 265–285.

Elvidge, C.D., 1990. Visible and near infrared reflectance characteristics of dry plant materials. Int. J. Remote Sens. 11, 1775–1795. https://doi.org/10.1080/01431169008955129.

Fabre, S., Lesaignoux, A., Olioso, A., Briottet, X., 2011. Influence of water content on spectral reflectance of leaves in the 3–15 μm domain. IEEE Geosci. Remote Sens. Lett. 8, 143–147.

Francois, C., Ottle, C., Prevot, L., 1997. Analytical parameterization of canopy directional emissivity and directional radiance in the thermal infrared. Application on the retrieval of soil and foliage temperatures using two directional measurements. Int. J.

Remote Sens. 18, 2587–2621. https://doi.org/10.1080/014311697217495.
Gates, D.M., Tantraporn, W., 1952. The reflectivity of deciduous trees and herbaceous plants in the infrared to 25 microns. Science 115, 613–616 80-.
Gates, D.M., Keegan, H.J., Schleter, J.C., Weidner, V.R., 1965. Spectral properties of plants. Appl. Opt. 4, 11–20. https://doi.org/10.1364/AO.4.000011.
Gerber, F., Marion, R., Olioso, A., Jacquemoud, S., Ribeiro da Luz, B., Fabre, S., 2011. Modeling directional-hemispherical reflectance and transmittance of fresh and dry leaves from 0.4μm to 5.7μm with the PROSPECT-VISIR model. Remote Sens. Environ. 115, 404–414. https://doi.org/10.1016/j.rse.2010.09.011.
Gobron, N., Pinty, B., Verstraete, M.M., Govaerts, Y., 1997. A semidiscrete model for the scattering of light by vegetation. J. Geophys. Res. Atmos. 102, 9431–9446. https://doi.org/10.1029/96JD04013.
Hecker, C., Hook, S., van der Meijde, M., Bakker, W., van Werff, H., Wilbrink, H., van Ruitenbeek, F., de Smeth, B., van der Meer, F., 2011. Thermal infrared spectrometer for earth science remote sensing applications-instrument modifications and measurement procedures. Sensors 11, 10981–10999. https://doi.org/https://doi.org/10.3390/s111110981.
Heredia-guerrero, J.A., Benítez, J.J., Domínguez, E., Bayer, I.S., 2016. Infrared spectroscopy as a tool to study plant cuticles. Spectrosc. Eur. 28.
Holloway, P.J., 1982. Structure and histochemistry of plant cuticular membranes: An overview. In: Cutler, D.F., Alvin, K.L., Price, C.E. (Eds.), The Plant Cuticle. Academic Press, London, pp. 1–32.
Hook, S.J., Johnson, W.R., Abrams, M.J., 2013. NASA's hyperspectral thermal emission spectrometer (HyTES), in: Kuenzer, C., Dech, S. (Eds.), Thermal Infrared Remote Sensing: Sensors, Methods, Applications, Remote Sensing and Digital Image Processing. Springer, Dordrecht, pp. 93–115. https://doi.org/https://doi.org/10.1007/978-94-007-6639-6.
Horler, D.N.H., Dockray, M., Barber, J., 1983. The red edge of plant leaf reflectance. Int. J. Remote Sens. 4, 273–288. https://doi.org/10.1080/01431168308948546.
Hulley, G.C., Hook, S.J., 2011. Generating consistent land surface temperature and emissivity products between ASTER and MODIS data for earth science research. IEEE Trans. Geosci. Remote Sens. 49, 1304–1315. https://doi.org/10.1109/TGRS.2010.2063034.
Hulley, G.C., Hook, S.J., Fisher, J.B., Lee, C.M., 2017. Ecostress, a NASA earth-ventures instrument for studying links between the water cycle and plant health over the diurnal cycle, in: IEEE International Geoscience and Remote Sensing Symposium (IGARSS). pp. 5494–5496. https://doi.org/https://doi.org/10.1109/IGARSS.2017.8128248.
Hunt Jr, E.R., Rock, B.N., 1989. Detection of changes in leaf water content using Near-and Middle-Infrared reflectances. Remote Sens. Environ. 30 (1), 43–54. https://doi.org/10.1016/0034-4257(89)90046-1.
Iaquinta, J., Pinty, B., 1997. Adaptation of a bidirectional reflectance model including the hot-spot to an optically thin canopy. Remote Sens. Rev. 15, 195–222. https://doi.org/10.1080/02757259709532338.
Jacob, F., Lesaignoux, A., Olioso, A., Weiss, M., Caillault, K., Jacquemoud, S., Nerry, F., French, A., Schmugge, T., Briottet, X., Lagouarde, J.P., 2017. Reassessment of the temperature-emissivity separation from multispectral thermal infrared data: introducing the impact of vegetation canopy by simulating the cavity effect with the SAIL-Thermique model. Remote Sens. Environ. 198, 160–172. https://doi.org/10.1016/j.rse.2017.06.006.
Jacquemoud, S., Bacour, C., Poilvé, H., Frangi, J.P., 2000. Comparison of four radiative transfer models to simulate plant canopies reflectance: direct and inverse mode. Remote Sens. Environ. 74, 471–481. https://doi.org/https://doi.org/10.1016/S0034-4257(00)00139-5.
Kampe, T.U., Johnson, B.R., Kuester, M., Keller, M., 2010. NEON: the first continental-scale ecological observatory with airborne remote sensing of vegetation canopy biochemistry and structure. J. Appl. Remote. Sens. 4. https://doi.org/https://doi.org/10.1117/1.3361375.
Kozhoridze, G., Orlovsky, N., Orlovsky, L., Blumberg, D.G., Golan-goldhirsh, A., 2016. Remote sensing models of structure-related biochemicals and pigments for classification of trees. Remote Sens. Environ. 186, 184–195. https://doi.org/10.1016/j.rse.2016.08.024.
Kuusk, A., 1995. A fast, invertible canopy reflectance model. Remote Sens. Environ. 51, 342–350. https://doi.org/10.1016/0034-4257(94)00059-V.
Lawrence, R., Labus, M., 2003. Early detection of Douglas-Fir beetle infestation with subcanopy resolution hyperspectral imagery. J. Appl. For. 18, 1–5.
Lee, C.M., Cable, M.L., Hook, S.J., Green, R.O., Ustin, S.L., Mandl, D.J., Middleton, E.M., 2015. An introduction to the NASA hyperspectral InfraRed imager (HyspIRI) mission and preparatory activities. Remote Sens. Environ. 167, 6–19. https://doi.org/10.1016/j.rse.2015.06.012.
Li, Z.-L., Wu, H., Wang, N., Qiu, S., Sobrino, J.A., Wan, Z., Tang, B.-H., Yan, G., 2013. Land surface emissivity retrieval from satellite data. Int. J. Remote Sens. 34, 3084–3127. https://doi.org/10.1080/01431161.2012.716540.
Meerdink, S.K., Roberts, D.A., King, J.Y., Roth, K.L., Dennison, P.E., Amaral, C.H., Hook, S.J., 2016. Linking seasonal foliar traits to VSWIR-TIR spectroscopy across California ecosystems. Remote Sens. Environ. 186, 322–338. https://doi.org/10.1016/j.rse.2016.08.003.
Meerdink, S., Roberts, D.A., Hulley, G., Pisek, J., Raabe, K., King, J., Hook, S.J., 2019. Plant species' spectral emissivity and temperature using the hyperspectral thermal emission spectrometer (HyTES) sensor. Remote Sens. Environ. 224, 421–435. https://doi.org/https://doi.org/10.1016/j.rse.2019.02.009.
Mitraka, Z., Chrysoulakis, N., Kamarianakis, Y., Partsinevelos, P., Tsouchlaraki, A., 2012. Improving the estimation of urban surface emissivity based on sub-pixel classification of high resolution satellite imagery. Remote Sens. Environ. 117, 125–134. https://doi.org/10.1016/j.rse.2011.06.025.
Okin, G.S., Roberts, D. a., Murray, B., Okin, W.J., 2001. Practical limits on hyperspectral vegetation discrimination in arid and semiarid environments. Remote Sens. Environ. 77, 212–225. https://doi.org/10.1016/S0034-4257(01)00207-3.
Olioso, A., 1995. Simulating the relationship between thermal emissivity and the normalized difference vegetation index. Int. J. Remote Sens. 16, 3211–3216. https://doi.org/10.1080/01431169508954625.
Ollinger, S.V., 2011. Sources of variability in canopy reflectance and the convergent properties of plants. New Phytol. 189, 375–394. https://doi.org/10.1111/j.1469-8137.2010.03536.x.
Riaño, D., Chuvieco, E., Ustin, S.L., Zomer, R., Dennison, P.E., Roberts, D.A., Salas, J., 2002. Assessment of vegetation regeneration after fire through multitemporal analysis of AVIRIS images in the Santa Monica Mountains. Remote Sens. Environ. 79, 60–71.
Ribeiro Da Luz, B., Crowley, J.K., 2007. Spectral reflectance and emissivity features of broad leaf plants: prospects for remote sensing in the thermal infrared (8.0–14.0 μm). Remote Sens. Environ. 109, 393–405. https://doi.org/10.1016/j.rse.2007.01.008.
Ribeiro Da Luz, B., Crowley, J.K., 2010. Identification of plant species by using high spatial and spectral resolution thermal infrared (8.0–13.5μm) imagery. Remote Sens. Environ. 114, 404–413. https://doi.org/10.1016/j.rse.2009.09.019.
Roberts, D.A., Smith, M.O., Adams, J.B., 1993. Green vegetation, nonphotosynthetic vegetation, and soils in AVIRIS data. Remote Sens. Environ. 44, 255–269. https://doi.org/10.1016/0034-4257(93)90020-X.
Roberts, D.A., Gardner, M., Church, R., Ustin, S.L., Scheer, G., 1998. Mapping chaparral in the Santa Monica Mountains using multiple endmember spectral mixture models. Remote Sens. Environ. 65, 267–279.
Roberts, D.A., Dennison, P.E., Gardner, M.E., Hetzel, Y., Ustin, S.L., Lee, C.T., 2003. Evaluation of the potential of hyperion for fire danger assessment by comparison to the airborne visible/infrared imaging spectrometer. IEEE Trans. Geosci. Remote Sens. 41, 1297–1310.
Roberts, D.A., Ustin, S.L., Ogunjemiyo, S., Greenberg, J., Dobrowski, Z., Chen, J., Hinckley, T.M., Dobrowski, S.Z., 2004. Spectral and structural measures of northwest Forest vegetation at leaf to landscape scales. Ecosystems 7, 545–562.
Saitoh, N., Imasu, R., Ota, Y., Niwa, Y., 2009. CO2 retrieval algorithm for the thermal infrared spectra of the greenhouse gases observing satellite: potential of retrieving CO2 vertical profile from high-resolution FTS sensor. J. Geophys. Res. Atmos. 114, 1–16. https://doi.org/https://doi.org/10.1029/2008JD011500.
Salisbury, J.W., 1986. Preliminary measurements of leaf spectral reflectance in the 8-14 mu-m region. Int. J. Remote Sens. 7, 1879–1886.
Salisbury, J.W., Milton, N.M., 1988. Thermal infrared (2.5 to 13.5 um) direction hemispherical reflectance of leaves. Photogramm. Eng. Remote. Sens. 54, 1301–1304.
Schimel, D.S., Pavlick, R., Fisher, J.B., Asner, G.P., Saatchi, S., Townsend, P.A., Miller, C., Frankenberg, C., Hibbard, K., Cox, P., 2014. Observing terrestrial ecosystems and the carbon cycle from space. Glob. Chang. Biol. 21, 1762–1776. https://doi.org/10.1111/gcb.12822.
Serbin, S.P., Singh, A., McNeil, B.E., Kingdon, C.C., Townsend, P.a., 2014. Spectroscopic determination of leaf morphological and biochemical traits for northern temperate and boreal tree species. Ecol. Appl. 24, 1651–1669. https://doi.org/10.1890/13-2110.1.
Snyder, W.C., Wan, Z., 1998. BRDF models to predict spectral reflectance and emissivity in the thermal infrared. IEEE Trans. Geosci. Remote Sens. 36, 214–225. https://doi.org/https://doi.org/10.1109/36.655331.
Stuffler, T., Kaufmann, C., Hofer, S., Förster, K.P., Schreier, G., Mueller, a., Eckardt, a., Bach, H., Penné, B., Benz, U., Haydn, R., 2007. The EnMAP hyperspectral imager—an advanced optical payload for future applications in earth observation programmes. Acta Astronaut. 61, 115–120. https://doi.org/https://doi.org/10.1016/j.actaastro.2007.01.033.
Ullah, S., Schlerf, M., Skidmore, A.K., Hecker, C., 2012a. Identifying plant species using mid-wave infrared (2.5–6μm) and thermal infrared (8–14μm) emissivity spectra. Remote Sens. Environ. 118, 95–102. https://doi.org/10.1016/j.rse.2011.11.008.
Ullah, S., Skidmore, A.K., Naeem, M., Schlerf, M., 2012b. An accurate retrieval of leaf water content from mid to thermal infrared spectra using continuous wavelet analysis. Sci. Total Environ. 437, 145–152.
Underwood, E., Ustin, S.L., DiPietro, D., 2003. Mapping nonnative plants using hyperspectral imagery. Remote Sens. Environ. 86, 150–161. https://doi.org/https://doi.org/10.1016/S0034-4257(03)00096-8.
Ustin, S.L., Gamon, J.A., 2010. Remote sensing of plant functional types. New Phytol. 795–816. https://doi.org/10.1111/j.1469-8137.2010.03284.x.
van der Meer, F.D., van der Werff, H.M.A., van Ruitenbeek, F.J.A., Hecker, C.A., Bakker, W.H., Noomen, M.F., van der Meijde, M., Carranza, E.J.M., de Smeth, J.B., Woldai, T., 2012. Multi- and hyperspectral geologic remote sensing: a review. Int. J. Appl. Earth Obs. Geoinf. 14, 112–128. https://doi.org/https://doi.org/10.1016/j.jag.2011.08.002.
Veraverbeke, S., Hook, S.J., Harris, S., 2012. Synergy of VSWIR (0.4-2.5μm) and MTIR (3.5-12.5μm) data for post-fire assessments. Remote Sens. Environ. 124, 771–779. https://doi.org/10.1016/j.rse.2012.06.028.
Verhoef, W., 1984. Light scattering by leaf layers with application to canopy reflectance modeling: the SAIL model. Remote Sens. Environ. 16, 125–141. https://doi.org/10.1016/0034-4257(84)90057-9.
Verhoef, W., Jia, L., Xiao, Q., Su, Z., 2007. Unified optical-thermal four-stream radiative transfer theory for homogeneous vegetation canopies. IEEE Trans. Geosci. Remote Sens. 45, 1808–1822. https://doi.org/10.1109/TGRS.2007.895844.
Wetherley, E.B., Roberts, D.A., McFadden, J., 2017. Mapping spectrally similar urban materials at sub-pixel scales. Remote Sens. Environ. 195, 170–183. https://doi.org/10.1016/j.rse.2017.04.013.
Wong, C., Blevin, W., 1967. Infrared reflectances of plant leaves. Aust. J. Biol. Sci. 20, 501. https://doi.org/10.1071/BI9670501.
Woolley, J.T., 1971. Reflectance and transmittance of light by leaves. Plant Physiol. 47, 656–662. https://doi.org/10.1104/pp.47.5.656.